Supplementary Information

Dispersal mode and spatial heterogeneity shape the interaction between adaptation and dispersal in multitrophic metacommunities

Pablo Moisset de Espanés, Ana I. Borthagaray, Matías Arim and Rodrigo Ramos-Jiliberto

1 Supplementary Methods

1.1 The dynamic model

We follow the allometric trophic network (ATN) model and parameterization of [2], extended to metacommunities. The resulting model consists of differential equations for the biomass of species i at site k, $B_{i,k}$, and for its average physiologically optimal temperature, $W_{i,k}$:

$$\dot{B}_{i,k} = \hat{r}_{i,k} G_{i,k} B_{i,k} - x_{i,k} B_{i,k} + B_{i,k} \sum_j F_{ji,k} \hat{e}_{ji,k} - \sum_j B_{j,k} F_{ij,k} - B_{i,k} \sum_l D_{i,kl} + \sum_l D_{i,lk} B_{i,l} \tag{1}$$

$$\dot{W}_{i,k} = \kappa_i^{\mathrm{W}} \cdot s_{i,k,\epsilon}^{\mathrm{W}}(W_{i,k}, \varphi_{i,k}^{\mathrm{W}}) \varphi_{i,k}^{\mathrm{W}} + \frac{1}{B_{i,k}} \left[\sum_l (W_{i,l} - W_{i,k}) D_{i,lk} B_{i,l} \right] \tag{2}$$

The first term of Eq. (1) is the logistic growth expression for plants, where

$$G_{i,k} = 1 - \frac{\sum_j \alpha_{ij} B_{j,k}}{K_{i,k}} \tag{3}$$

The second term is the metabolic loss. The third and fourth terms are the biomass intake/loss due to trophic interactions, whose functional responses are:

$$F_{ij,k} = \frac{a_{ij,k} B_{i,k}}{1 + c_{j,k} B_{j,k} + \sum_l h_{lj} a_{lj,k} B_{l,k}} \tag{4}$$

Both plants' specific growth rates $\hat{r}_{i,k}$ and animals' conversion efficiencies $\hat{e}_{ij,k}$ are

$$\hat{r}_{i,k} = r_{i,k} \ \rho(W_{i,k}, T_k(t)) \tag{5}$$

$$\hat{e}_{ij,k} = e_{ij} \ \rho(W_{j,k}, T_k(t)) \tag{6}$$

where function ρ captures how temperature adaptation affects these rates. Inspired by [4], we define

$$\rho(W,T) = \begin{cases} \exp\left(-\left(\frac{T-W}{2\sigma}\right)^2\right) & T \leq W \\ 1 - \left(\frac{T-W}{T_{\max}-W}\right)^2 & W < T \leq T_{\max} \\ 0 & T > T_{\max} \end{cases} \tag{7}$$

where $\sigma = (W - 273.15)/4.1$ and $T_{\max} = W + 10.2$, in Kelvin. Thus, ρ can be rewritten as

$$\rho(W,T) = \begin{cases} \exp\left(-\frac{1}{(2/4.1)^2}\left(1 - \frac{T-273.15}{W-273.15}\right)^2\right) & T \leq W \\ 1 - \left(\frac{T-W}{10.2}\right)^2 & W < T \leq T_{\max} \\ 0 & T > T_{\max} \end{cases} \tag{8}$$

The last two terms of Eq. (1) represent the biomass dispersal from/into site k. Factor $D_{i,kl}$ is the dispersal rate of species i from site k to site l. Our extension to multi-site landscapes includes a continuum between passive dispersal and source-fitness-dependent dispersal among sites. We measure fitness Q of species i as the per-capita growth rate at site k, neglecting dispersal.

$$Q_{i,k} = \hat{r}_{i,k} G_{i,k} - x_{i,k} + \sum_j F_{ji,k} \hat{e}_{ji} - \sum_j B_{j,k} F_{ij,k} / B_{i,k} \tag{9}$$

The propensity of individuals of species i to leave a site k is denoted as $f_i(Q_{i,k})$, where

$$f_i(Q) = \mathcal{H}(-Q) \cdot Q / (-Q_i^0 + Q) \tag{10}$$

and $\mathcal{H}$ is the Heaviside function. If $Q_{i,k} \geq 0$, no outflow of species i from site k occurs (i.e. $f_i(Q_{i,k}) = 0$). If $Q_{i,k} < 0$, the more negative $Q_{i,k}$ is, the faster the outflow rate from site k will be. Function $f_i(Q_{i,k})$ saturates to 1 as $Q_{i,k} \to -\infty$ and the saturation rate is modulated by positive parameter Q_i^0. The degree of fitness-dependency of dispersal rate is controlled by parameter $\beta_i \in [0, 1]$.

$$D_{i,kl} = (\beta_i f_i(Q_{i,k}) + (1 - \beta_i))D_i^\star / d_{kl} \tag{11}$$

where positive real $D_i^\star = D_0 M_i^{b_D}$ is the dispersal rate for species i between a pair of adjacent site k and l when $\beta = 0$ and the distance between the sites (d_{kl}) is one. M_i is the body mass of species i. Also, our model assumes that the dispersal rate is inversely proportional to the distance between adjacent sites. Summarizing, in this formulation, fitness dependence affects the propensity of individuals to leave the source site, whereas the distribution of movement among adjacent sites is modulated by inter-site distance. Thus, the model captures condition-dependent emigration from the source site rather than explicit destination choice based on habitat quality.

Regarding Eq. (2), the first term represents the adaptation process by which species i adjusts it optimal temperature $W_{i,k}$ following the fitness gradient $\varphi_{i,k}^{\mathrm{W}}$ defined as:

$$\varphi_{i,k}^{\mathrm{W}} = \frac{\partial Q_{i,k}}{\partial W_{i,k}} = \frac{\partial \rho(W_{i,k}, T_k)}{\partial W_{i,k}} \left(r_{i,k} G_{i,k} + \sum_j F_{ji,k} e_{ji} \right) \tag{12}$$

where

$$\frac{\partial \rho(W,T)}{\partial W} = \begin{cases} -\exp\left(-\frac{1}{(2/4.1)^2}\left(1 - \frac{T-273.15}{W-273.15}\right)^2\right) \frac{2}{(2/4.1)^2} \frac{(W-T)(T-273.15)}{(W-273.15)^3} & T \leq W \\ \frac{2}{10.2^2}(T-W) & W < T \leq T_{\max} \\ 0 & T > T_{\max} \end{cases} \tag{13}$$

The first term of Eq. (2) also contains the factor $s_{i,k,\epsilon}^{\mathrm{W}}(W_{i,k}, \varphi_{i,k}^{\mathrm{W}})$, whose purpose is to constrain the values of $W_{i,k}$ to the $[W_{i,k}^{\min}, W_{i,k}^{\max}]$ interval. In particular

$$s_{i,k,\epsilon}^{\mathrm{W}}(W, \varphi) = \hat{s}_\epsilon \left(\frac{W - W_{i,k}^{\min}}{W_{i,k}^{\max} - W_{i,k}^{\min}}, \varphi \right) \tag{14}$$

where

$$\hat{s}_\epsilon(z, \varphi) = \begin{cases} 1 & \varphi > 0, z \leq 1 - \epsilon. \\ \frac{1-z}{\epsilon} & \varphi > 0, z > 1 - \epsilon. \\ 1 & \varphi \leq 0, z > \epsilon \\ \frac{z}{\epsilon} & \varphi \leq 0, z \leq \epsilon \end{cases} \tag{15}$$

The second term of Eq. (2) represents the change in $W_{i,k}$ due to the averaging process between residents of site k and the incoming individuals from neighboring sites l. To derive this term, consider a simpler system consisting of a single species with biomass B_0 with a W_0 value at site 0. Call ΔB_i the biomass arriving from site $i \neq 0$ and call W_i its trait value. The new W value for site 0 is the average of trait values (W_0, W_i) weighted with the corresponding B_0 and ΔB_i's. Therefore,

$$W = \frac{W_0 B_0 + \sum_i W_i \Delta B_i}{B_0 + \sum_i \Delta B_i} \tag{16}$$

which is analogous to the well-known Richmann's law of mixing components with different temperatures. To derive the second term of Eq. (2), we extend Eq. (16) to average the optimal temperature $W_{i,k}(t)$, considering

local dynamics $Q_{i,k}$, and the in/out biomass fluxes from/to neighboring sites during a time interval Δt. After a Δt time increment,

$$W_{i,k}(t+\Delta t) = \frac{\Delta t\ Q_{i,k}W_{i,k}(t) + \sum_l \Delta B_{i,lk}(t)W_{i,l}(t) - \sum_l \Delta B_{i,kl}(t)W_{i,k}(t) + B_{i,k}(t)W_{i,k}(t)}{\Delta t\ Q_{i,k} + \sum_l \Delta B_{i,lk}(t) - \sum_l \Delta B_{i,kl}(t) + B_{i,k}(t)} \tag{17}$$

Subtracting $W_{i,k}(t)$ from both sides, dividing by Δt and simplifying we obtain:

$$\frac{W_{i,k}(t+\Delta t) - W_{i,k}(t)}{\Delta t} = \frac{\sum_l \left(W_{i,l}(t) - W_{i,k}(t)\right) \Delta B_{i,lk}(t)/\Delta t}{\Delta t\ Q_{i,k} + \sum_l \Delta B_{i,lk}(t) - \sum_l \Delta B_{i,kl}(t) + B_{i,k}(t)} \tag{18}$$

Note that $\lim_{\Delta t\to 0} \Delta B_{i,lk}(t)/\Delta t = D_{i,lk}B_{i,l}$, because this limit represents the instantaneous influx of biomass from site l to site k. Then, the time derivative of $W_{i,k}(t)$ is

$$W'_{i,k}(t) = \lim_{\Delta t\to 0} \frac{W_{i,k}(t+\Delta t) - W_{i,k}(t)}{\Delta t} = \frac{1}{B_{i,k}(t)} \left[\sum_l \left(W_{i,l}(t) - W_{i,k}(t)\right) D_{i,lk}(t)B_{i,l}(t)\right] \tag{19}$$

which is the second term of Eq. (2).

Remark: More formally, instead of $\Delta B_{i,lk}(t)W_{i,l}(t)$ we should have written

$$\int_t^{t+\Delta t} D_{i,lk}(u)B_{i,l}(u)W_{i,l}(u)\,du = D_{i,lk}(t+\zeta)B_{i,l}(t+\zeta)W_{i,l}(t+\zeta)\Delta t \tag{20}$$

for some $\zeta \in (t, t+\Delta t)$. We would have arrived to Eqn. (19) although the derivation would have been more cumbersome.

1.2 Numerical considerations

Equation (2) presents problem in the reasonable case of some species i not being present at a site k. There is the conceptual issue of assigning a value to $W_{i,k}$. Although it may appear that this value is complete irrelevant (being species i absent), then there is the numerical problem of the denominator $B_{i,k}$ being zero. If there is a non-zero mass influx from a site l and $W_{i,l} \neq W_{i,k}$ then $\dot{W}_{i,k}$ becomes infinite. This reflects the fact that $W_{i,k}$ should adopt instantaneously the value $W_{i,l}$, because the average optimal temperature is determined only by the incoming individuals. To overcome this mathematical and numerical problem, we define a new variable $Y_{i,k} = B_{i,k} \cdot W_{i,k}$ and we rewrite the differential equations. Then

$$\dot{Y}_{i,k} = \dot{B}_{i,k} \cdot W_{i,k} + B_{i,k} \cdot \dot{W}_{i,k} \tag{21}$$

$$= \kappa_i^{\mathrm{W}} \cdot s_{i,k,\epsilon}^{\mathrm{W}}(W_{i,k}, \varphi_{i,k}^{\mathrm{W}})\varphi_{i,k}^{\mathrm{W}}B_{i,k} + \left[\sum_l \left(W_{i,l} - W_{i,k}\right) D_{i,lk}B_{i,l}\right] + \dot{B}_{i,k} \cdot W_{i,k} \tag{22}$$

This representation avoids the division by zero. However, we still need to compute the actual W values to evaluate, for example, ρ. Although $W_{i,k} = Y_{i,k}/B_{i,k}$ is indeed indeterminate when $B_{i,k} = 0$, this is easily overcome by using $W_{i,k} = Y_{i,k}/(B_{i,k} + \varepsilon)$, where ε is a small value.

1.3 Parameterization

For processes occurring within single communities, we followed [1], modified by [2]. For the dispersal and adaptation processes, we either fixed the parameters to reasonable values or we explored a wide interval. For details, see Table 1.

$$M_i = m_0 \mathcal{Z}^{\mathrm{TL}(i)+\tau} \tag{23}$$

$$r_{i,k} = r_0 M_i^{b_\mathrm{r}} \eta_\mathrm{r}(T_k) \tag{24}$$

$$x_{i,k} = x_0 M_i^{b_\mathrm{x}} \eta_\mathrm{x}(T_k) \tag{25}$$

$$a_{ij,k} = a_0 M_i^{b_\mathrm{a}} M_j^{c_\mathrm{a}} \eta_\mathrm{a}(T_k) \tag{26}$$

$$h_{ij} = h_0 M_i^{b_\mathrm{h}} M_j^{c_\mathrm{h}} \eta_\mathrm{h}(T_k) \tag{27}$$

$$K_{i,k} = K_0 M_i^{b_\mathrm{K}} \eta_\mathrm{K}(T_k)\, \mathcal{U} \tag{28}$$

$$c_{i,k} = c_0 \eta_\mathrm{c}(T_k) \tag{29}$$

$$D_i^\star = D_0 M_i^{b_\mathrm{D}} \tag{30}$$

TL(i) is the trophic level of species i (TL = 0 for basals), and $\tau \sim U(-\omega, \omega)$. Functions η_* describe the temperature dependence of each parameter according to

$$\eta_*(T) = e^{E_* \frac{T_0 - T}{\kappa_t T T_0}} \tag{31}$$

where T is environmental temperature in Kelvin, E_* being activation energy of parameter $*$, $\kappa_t = 8.62 \cdot 10^{-5}$eV/K is the Boltzmann's constant. We added some differences in K among sites, to emulate heterogeneity in sites' productivity, with the random factor $\mathcal{U} \sim U(1, 1 + K_\mathrm{n})$.

Symbol	Value	Unit
r_0	exp(-15.68)	s^{-1}
x_0	exp (-16.54)	s^{-1}
a_0	exp(-13.1)	$m^2 s^{-1}$
h_0	exp(9.66)	s
b_r	-0.25	dl
b_x	-0.31	dl
b_K	0.28	dl
b_a	0.25	dl
b_h	-0.45	dl
c_a	-0.8	dl
c_h	0.47	dl
α_{ij}	1 for $i = j$, 0.2 else	dl
K_0	40	$g m^{-2}$
c_0	0.8	$g^{-1} m^{-2}$
E_K	0.71	eV
E_r	-0.84	eV
E_a	-0.38	eV
E_h	0.26	eV
E_x	-0.69	eV
E_c	-0.65	eV
e_i	0.545 (prey is a plant), 0.906 (prey is animal)	dl
T_0	293	K
m_0	0.001	g
$\mathcal{Z}$	10	dl
b_D	0.25 [1]	dl
Q_i^0	10^{-5}	s^{-1}
ϵ	0.1	dl
ω	0.1	dl
K_n	1	dl
$W_{i,k}^{min}$	273	K
$W_{i,k}^{max}$	313	K
β_i	free, in interval $[0, 1]$	dl
κ_i^W	free, in interval $[10^{-3}, 10^2]$	K^2
D_0	free, in interval $[10^{-8}, 10^{-4}]$	distance/(s g^{b_D})
T_{radius}	free, in interval $[0.5, 15]$	K
$T_k(t)$	free, in interval $293 \pm T_{radius}$	K

Supplementary Table 1: Parameter values used in our simulations. Values in upper section were taken from [2]. [1] from [3]

2 Supplementary Results

2.1 Varying the number of landscape sites

To show the influence of landscape structure on biodiversity patterns, we present in this section results for landscapes composed of 3, 12, 25 and 50 sites. In all cases the number of edges equals twice the number of sites, which preserves the mean degree of the landscape graph.

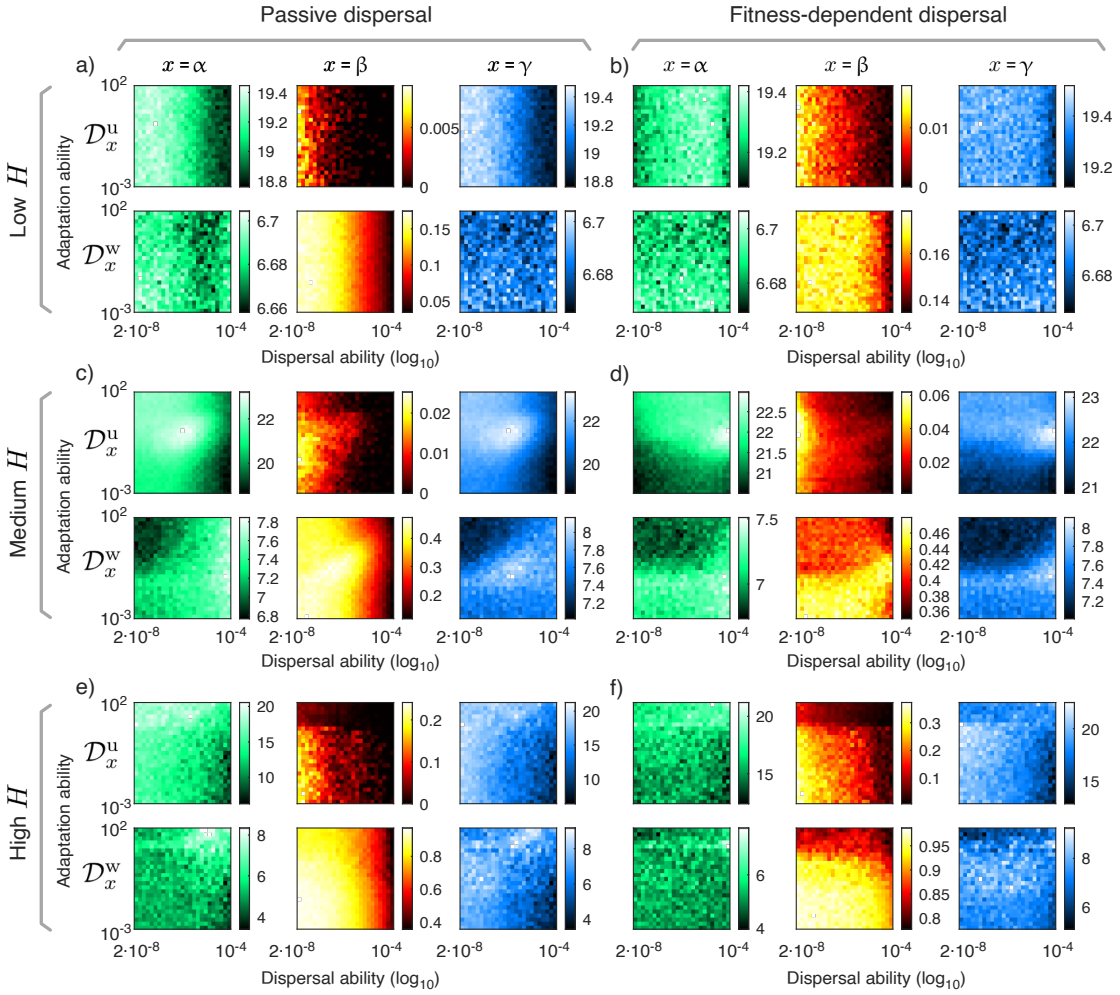

Supplementary Figure 1: **Results for 3-site landscapes.** Effects of dispersal and adaptation abilities on biodiversity patterns under passive (a, c, e) and fitness-dependent (b, d, f) dispersal across three levels of spatial heterogeneity: low (a, b), medium (c, d), and high (e, f). The landscapes consist of 3 sites and 3 edges. The food webs include 50 species with a connectance of 0.1. Each pixel represents the average of 50 replicates. $\mathcal{D}_x^{\mathrm{u}}$ and $\mathcal{D}_x^{\mathrm{w}}$ denote unweighted (presence-absence based) and abundance-weighted x-diversities, respectively, where $x = [\alpha, \beta, \gamma]$.

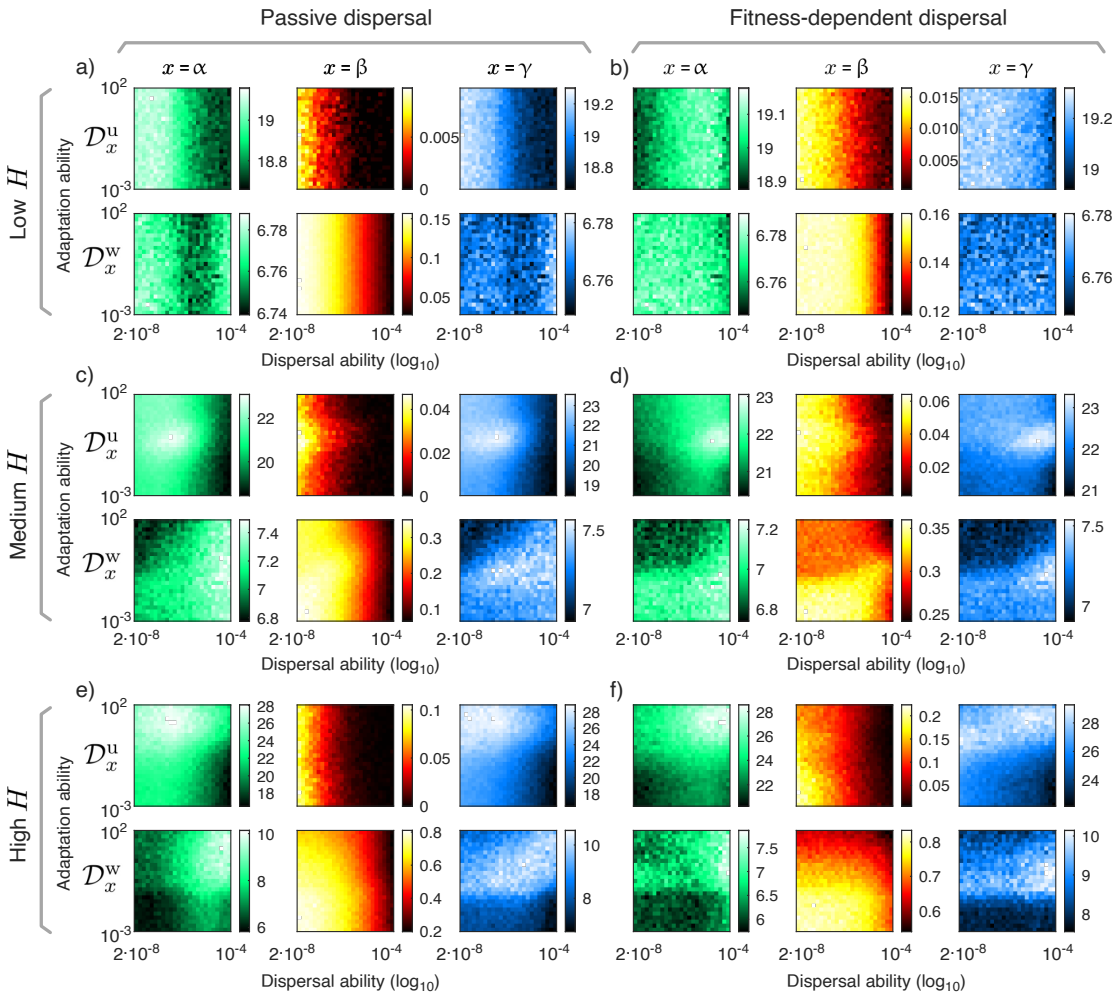

Supplementary Figure 2: **Results for 12-site landscapes.** All other parameters remain the same as those used in Fig. 1, except for the number of landscape edges, which is set to 24.

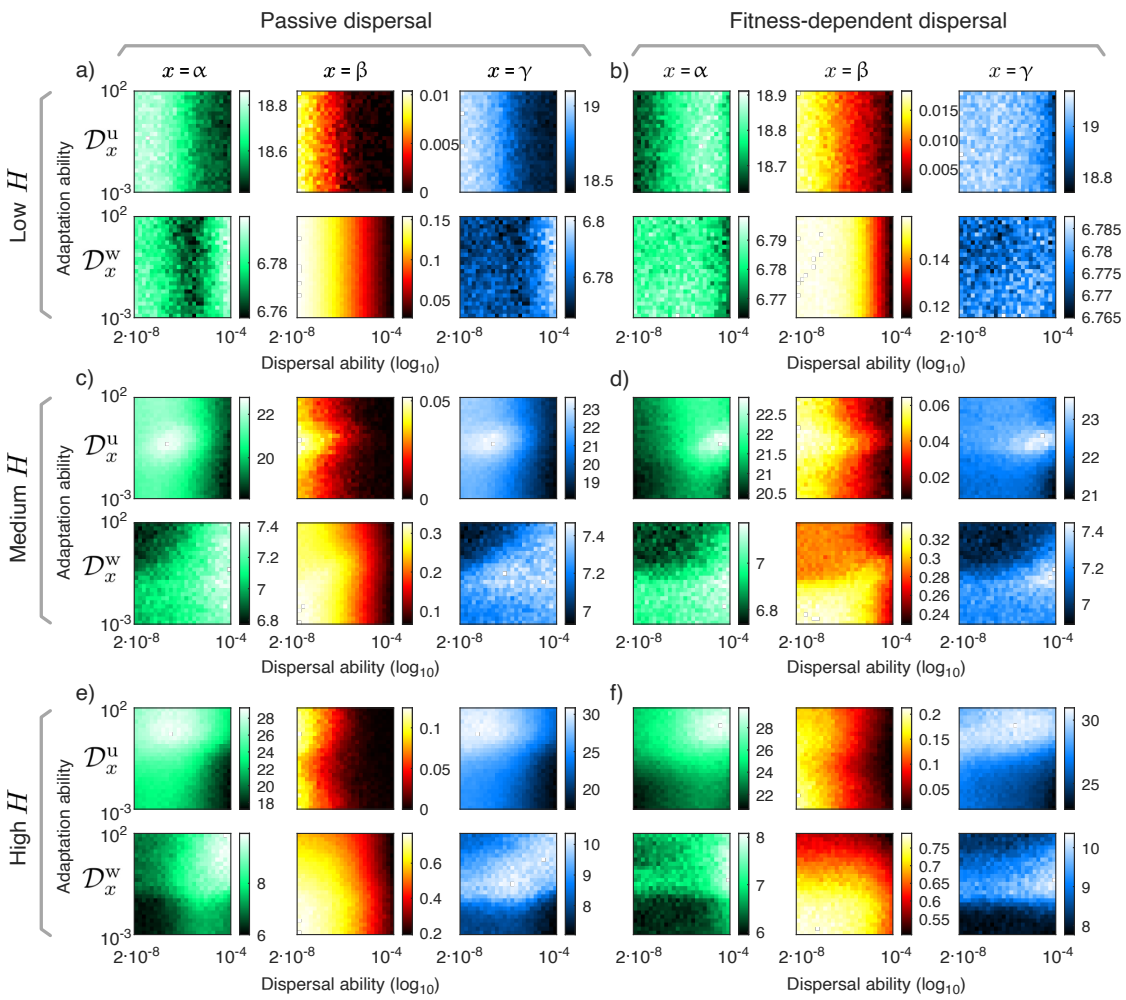

Supplementary Figure 3: **Results for 25-site landscapes.** All parameters are the same as those used in Fig. 1.

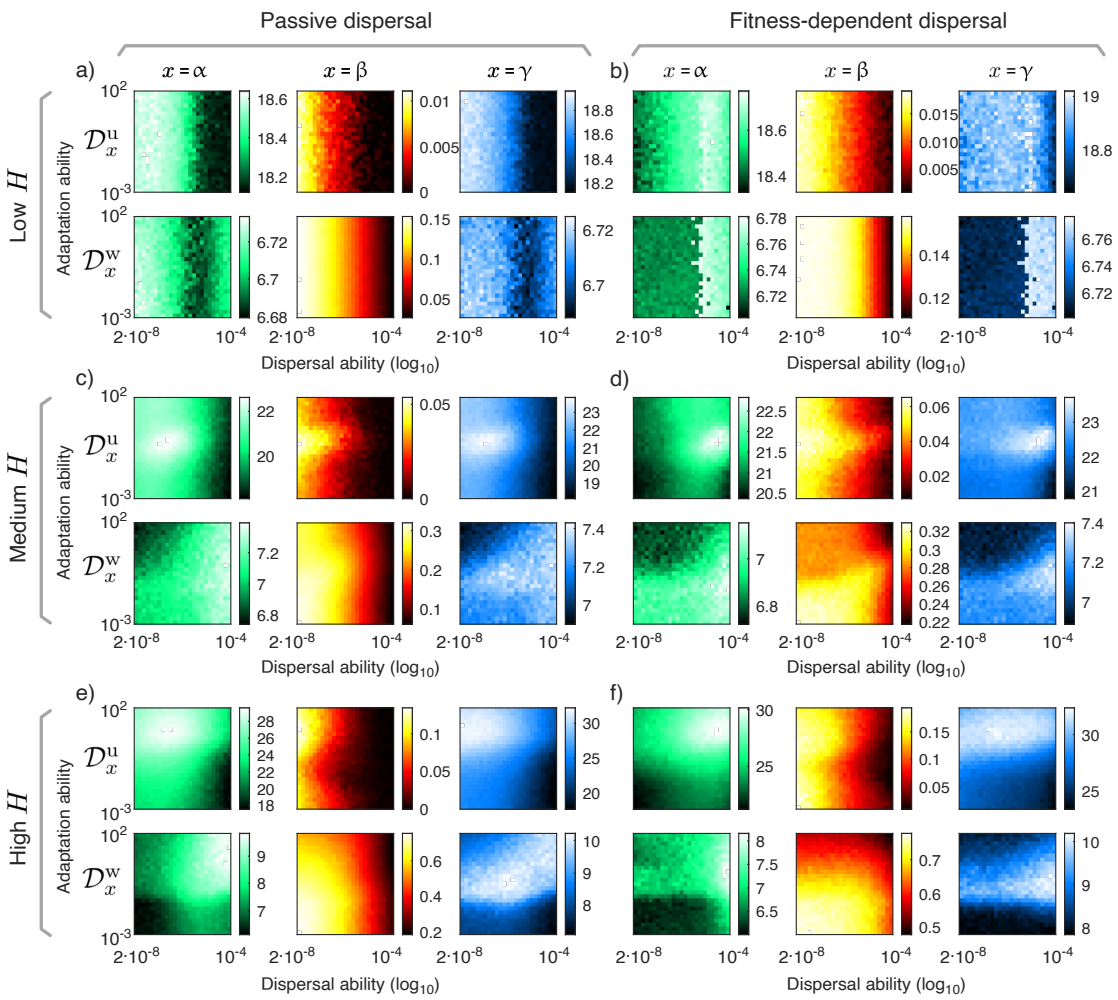

Supplementary Figure 4: **Results for 50-site landscapes.** All other parameters remain the same as those used in Fig. 1, except for the number of landscape edges, which is set to 100.

2.2 Varying the number of landscape edges

To show the influence of landscape structure on biodiversity patterns, we present in this section results for landscapes composed of 25 sites with 24, 50, 125 and 250 edges.

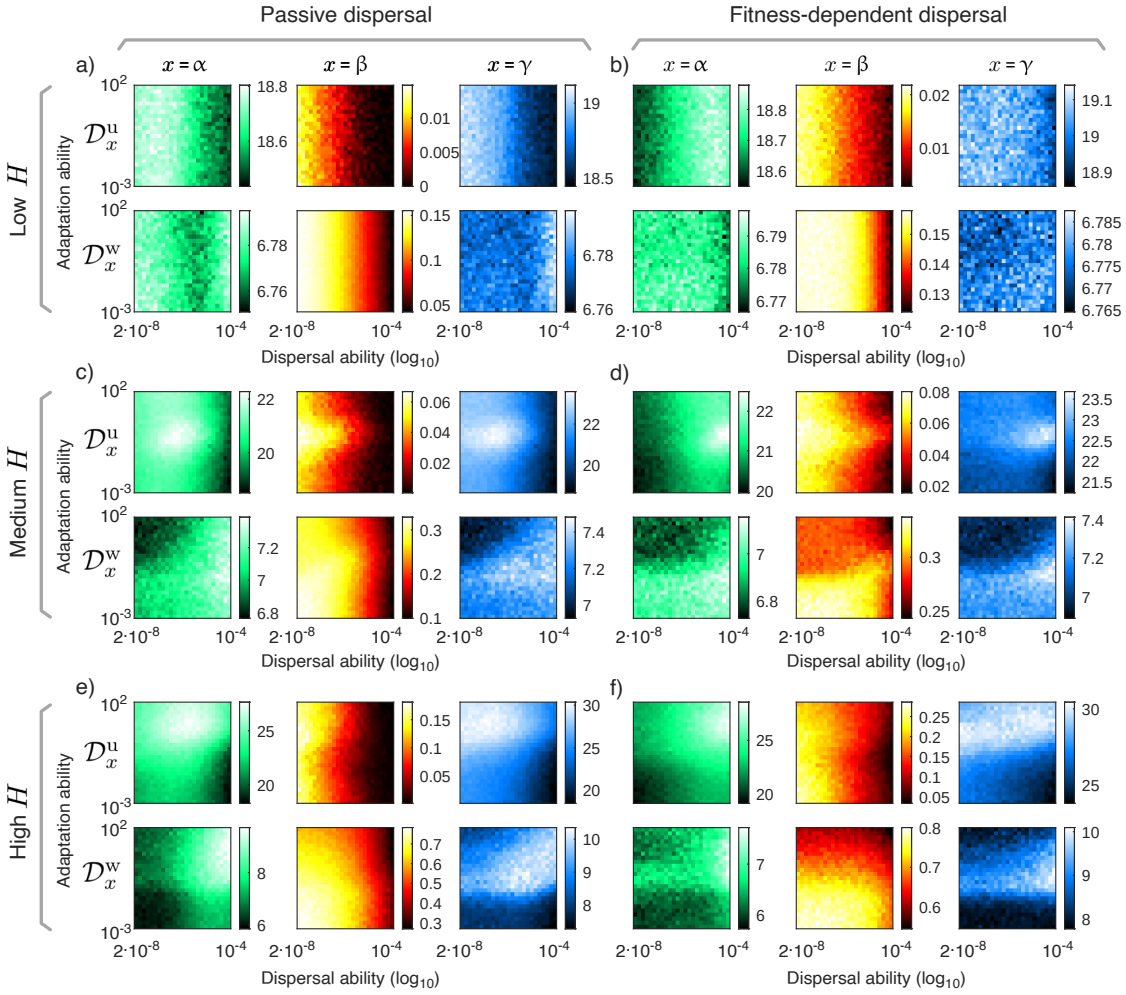

Supplementary Figure 5: **Results for 24-edge landscapes.** All other parameters remain the same as those used in Fig. 1, except for the number of landscape sites, which is set to 25.

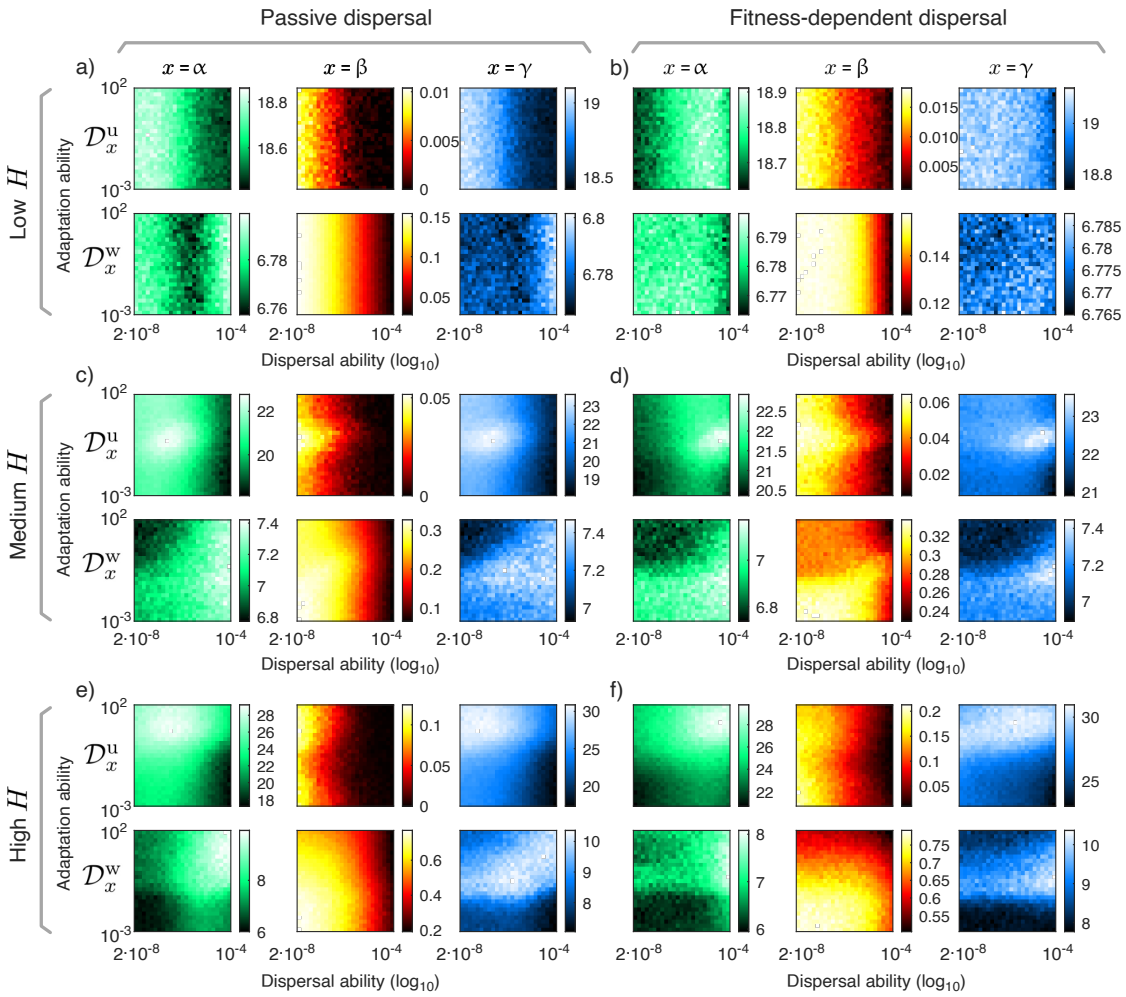

Supplementary Figure 6: **Results for 50-edge landscapes.** All other parameters remain the same as those used in Fig. 1, except for the number of landscape sites, which is set to 25.

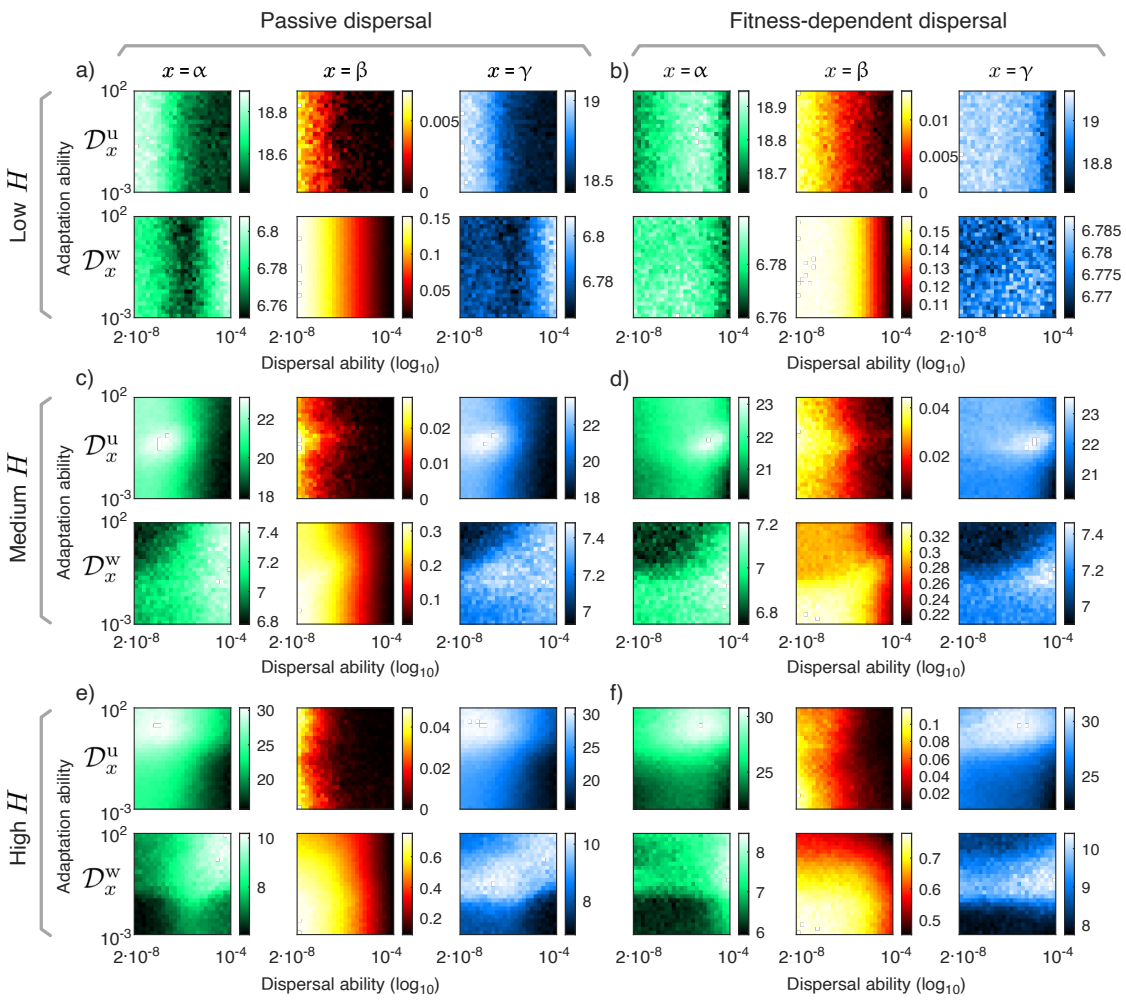

Supplementary Figure 7: **Results for 125-edge landscapes.** All other parameters remain the same as those used in Fig. 1, except for the number of landscape sites, which is set to 25.

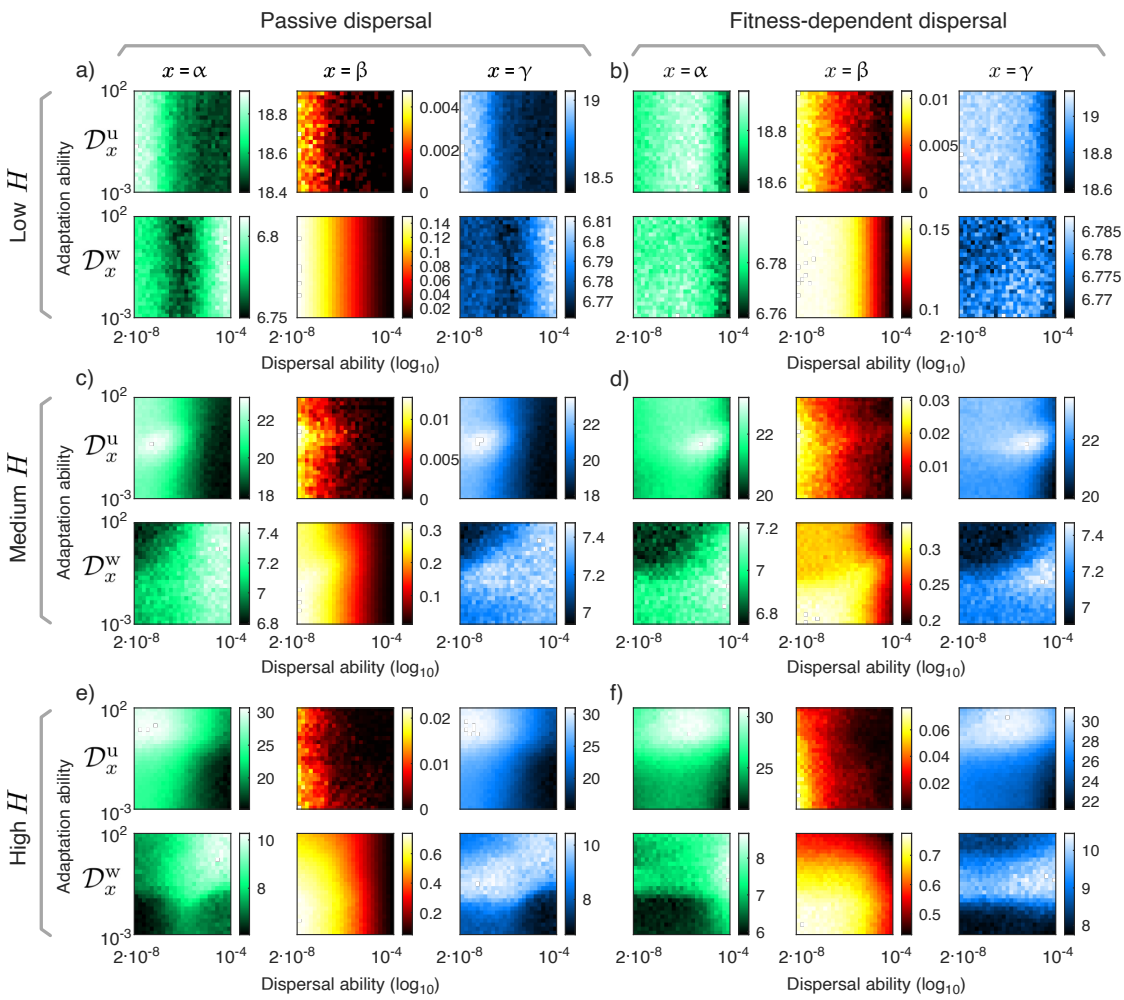

Supplementary Figure 8: **Results for 250-edge landscapes.** All other parameters remain the same as those used in Fig. 1, except for the number of landscape sites, which is set to 25.

2.3 Varying the width of the temperature-performance function

This figure shows the sensitivity of our results to changes in the width of the temperature-performance curve, governed by parameter σ in Eq. (7).

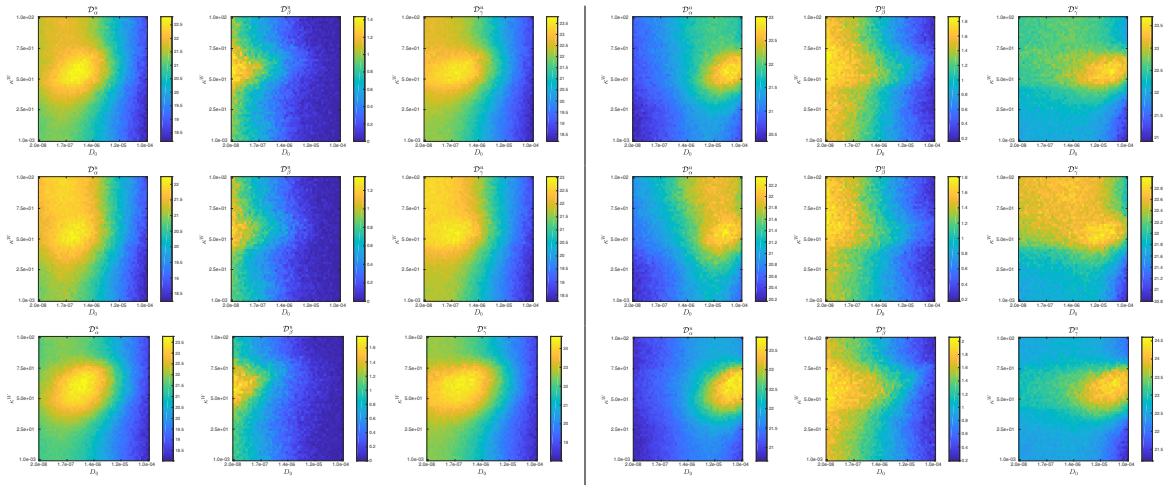

Supplementary Figure 9: Results for $\beta = 0$ (left) and $\beta = 0.99$ (right), with medium spatial heterogeneity, and with σ at its base value (top row), 3% above its base value (middle row) and 50% below its base value (bottom row).

2.4 Varying the spatial autocorrelacion of local conditions

This figure shows the sensitivity of our results to temperature autocorrelation, measured using the global Moran's I measure. The experiments used landscapes composed of 25 sites with 50 edges.

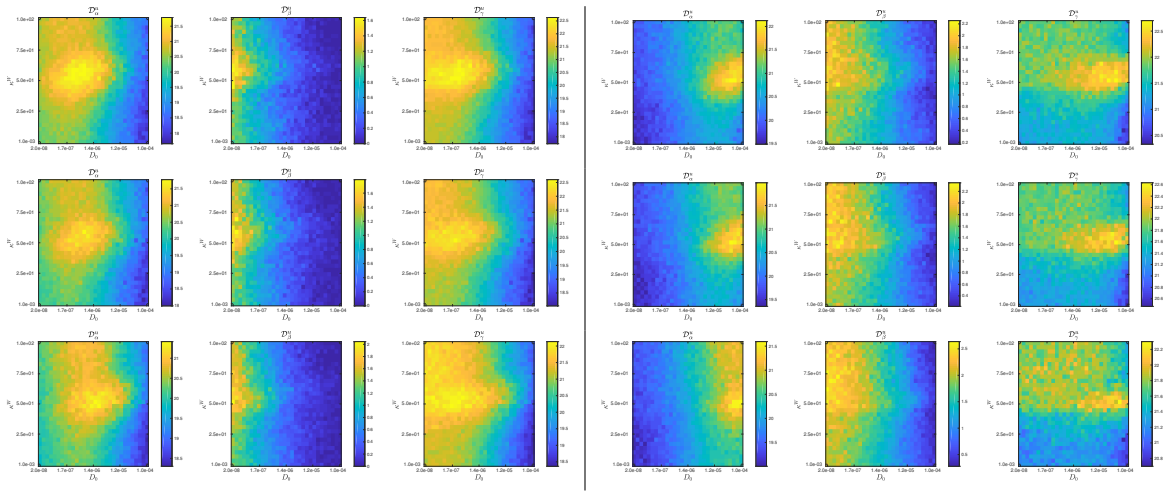

Supplementary Figure 10: Results for $\beta = 0$ (left) and $\beta = 0.99$ (right), with medium spatial heterogeneity, and with varying strength of spatial autocorrelation (SAC) in local temperatures. Top row: low SAC (global Moran I index = 0.19). Middle row: medium SAC (global Moran I index = 0.41). Bottom row: high SAC (global Moran I index = 0.72). The landscapes consist of 25 sites and 50 edges. The food webs include 50 species with a connectance of 0.1. Each pixel represents the average of 30 replicates.

2.5 Comparing competitive and multitrophic metacommunities

To compare our main results on multitrophic metacommunities with the behavior of competitive metacommunities, in Fig. 11a, c, e we present the simulation outcomes for communities lacking trophic structure, where all species compete both intra- and interspecifically. By contrast, in Fig. 11b, d, f, we present the simulation outcomes for communities with trophic structure, where only basal species compete both intra- and interspecifically. This was the setting for our main experiments. For all cases, the interspecific competition strength was drawn uniformly from the interval $[0, 0.2]$, while the intraspecific competition strength was fixed at 0.3. Additionally, we set $K_{i,k} = 0.01$ for all i in 25% of the landscape sites.

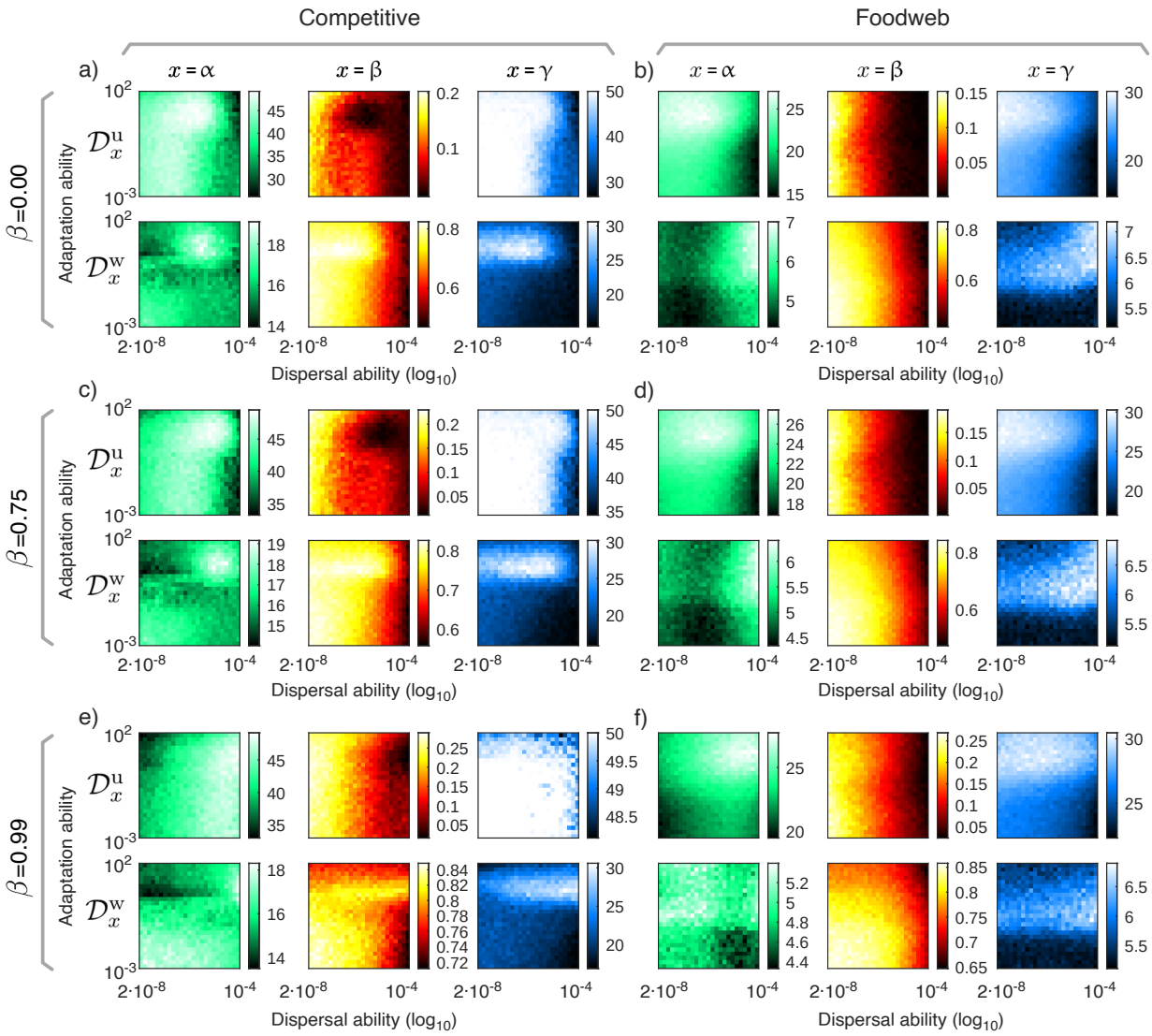

Supplementary Figure 11: Comparison between competitive and foodweb metacommunities with different dispersal modes. Fitness dependency of dispersal is either null with $\beta = 0$ (a, b), medium with $\beta = 0.75$ (c, d), and high with $\beta = 0.99$ (e, f). Initial species richness is 50. For foodwebs, trophic connectance is 0.1. The landscapes consist of 25 sites and 50 edges, while spatial heterogeneity H is set to high. Each pixel represents the average of 50 replicates. $\mathcal{D}_x^{\mathrm{u}}$ and $\mathcal{D}_x^{\mathrm{w}}$ denote unweighted (presence-absence based) and abundance-weighted x-diversities, respectively, where $x = [\alpha, \beta, \gamma]$.

Supplementary References

[1] Amrei Binzer, Christian Guill, Björn C Rall, and Ulrich Brose. Interactive effects of warming, eutrophication and size structure: impacts on biodiversity and food-web structure. *Global Change Biology*, 22(1):220–227, 2016.

[2] Benoit Gauzens, Ulrich Brose, Eva Delmas, and Emilio Berti. Atnr: Allometric trophic network models in r. *Methods in Ecology and Evolution*, 14(11):2766–2773, 2023.

[3] Esteban Ortiz, Ana I Borthagaray, Rodrigo Ramos-Jiliberto, and Matías Arim. Scaling of biological rates with body size as a backbone in the assembly of metacommunity biodiversity. *Biology Letters*, 19(6):20220618, 2023.

[4] Tyler Wagner, Erin M Schliep, Joshua S North, Holly Kundel, Christopher A Custer, Jenna K Ruzich, and Gretchen JA Hansen. Predicting climate change impacts on poikilotherms using physiologically guided species abundance models. *Proceedings of the National Academy of Sciences*, 120(15):e2214199120, 2023.